Machine Learning Approaches to Classify Anatomical Regions in Rodent Brain from High Density Recordings

Anna Windbühler[1,2], Sükrü Okkesim[1,3], Olaf Christ[1], Soheil Mottaghi[1], Shavika Rastogi[4,5], Michael Schmuker[5], Timo Baumann[2,6] and Ulrich G. Hofmann[1]
corresponding author: ulrich.hofmann@klinikum.uni-freiburg.de

***Abstract*— Identifying different functional regions during a brain surgery is a challenging task usually performed by highly specialized neurophysiologists. Progress in this field may be used to improve *in situ* brain navigation and will serve as an important building block to minimize the number of animals in preclinical brain research required by properly positioning implants intraoperatively. The study at hand aims to correlate recorded extracellular signals with the volume of origin by deep learning methods. Our work establishes connections between the position in the brain and recorded high-density neural signals. This was achieved by evaluating the performance of BLSTM, BGRU, QRNN and CNN neural network architectures on multisite electrophysiological data sets. All networks were able to successfully distinguish cortical and thalamic brain regions according to their respective neural signals. The BGRU provides the best results with an accuracy of 88.6 % and demonstrates that this classification task might be solved in higher detail while minimizing complex preprocessing steps.**

I. INTRODUCTION

Surgical interventions to the brain are considered to be among the most challenging medical procedures not the least due of the lack of clear and easy accessible landmarks. Yet, bioelectronic medicine offers a growing number of therapeutic avenues and as such creates a strong demand for precision implantations enabled by sophisticated imaging [1]. Unfortunately, pre-clinical research with rodents rarely provides for this luxuriousness and has to compensate for implantation errors by increasing the number of animals, even though robotized stereotaxic targeting becomes available [2]. To minimize animal use while increasing targetting precision, we propose a **functional atlas** based on intraoperatively acquired electrophysiology recordings to identify distinct brain regions instead of relying on their post-mortem stainings [3]. The challenge reminisces of constructing an atlas based on spoken languages and dialects in lieu of political borders and landmarks (see Figure 1). With the advent of an according functional brain atlas, a simple look-up for signal features might e.g. reveal sub-cortical nucleus' boundaries similar to human Deep Brain Stimulator implantation [4]. Microelectrode probes of different design and make are routinely used in animal research and might thus provide precise multisite extracellular recordings (MER) **attributable** to a corresponding brain location.

Fig. 1. Illustration of the proposed functional atlas: A traveler across Europe will often recognize political borders by the differences in local language along his path. Modified after Wikimedia Commons.

In the following work in progress, extracellular recordings from high density, silicon multi-site microelectrodes [5], [6] at different known, intracranial locations will be used as a proof of principle to harness the power of machine learning approaches and pave the way for such a functional brain map.

II. MATERIALS AND METHODS

Two different types of silicon probes were used to acquire the data sets for the classification tasks below. Recordings are real extracellular measurements with neuronal (micro-electrode) resolution from animals in vivo.

A. Animal procedures

Our own data set, called NES, was acquired as described in [5] with 1600 recording sites neural probes (EDC) from anesthetized, female Sprague Dawley rats with a weight of ca. 290 g each. Sampling rate was 5 kHz per site for blocks of 32 sites. All procedures involving animal experiments were conducted following the guidelines of the German Council on Animal Protection. The protocols were approved by the

[1]Neuroelectronic Systems, Department of Neurosurgery, University Medical Center Freiburg and Medical Faculty, University of Freiburg, DE
[2]Department of Informatics, Universität Hamburg, DE
[3]FRIAS - Freiburg Institute for Advanced Studies, Freiburg, DE
[4]International Centre for Neuromorphic Systems, The MARCS Institute of Brain, Behaviour and Development, Western Sydney University, Sydney, AUS
[5]Biocomputation Group, University of Hertfordshire, UK
[6]Faculty of Informatics and Mathematics, OTH Regensburg, DE

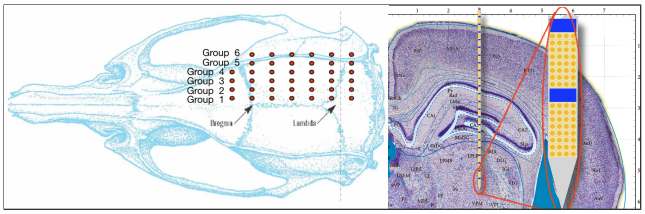

Fig. 2. (left) Designated trepanation positions on a typical rat skull. Clearly visible are Bregma and Lambda bone structures (arrows).
(right) To-scale illustration of an 100 µm wide EDC probe at hole number 4 (at 4 mm posterior Bregma) of group 3 (3 mm lateral midline) of a merged atlas slice. Pics modified from [8].

Animal Care Committee of the University of Freiburg under the supervision of the Regierungpräsidium Freiburg (approval 35-9185.81/G-13/01) in accordance with the guidelines of the European Union Directive 2010/63/UE. Female Sprague-Dawley rats (n = 6) underwent stereotactic surgery for acute implantation of EDC probes while anesthetized with Ketamin/Xylazine as described earlier [7].
An overview of designated trepanation positions is given in Figure 2 (left) with each position acquired on one single pass from at least three different rats. No single rat was used for more than four widely separated trepanation holes currently undersampling the originally intended number of trajectories.

B. Datasets

Dataset HC2 and HC4 are recordings from the Buzsáki-Lab, freely available on http://crcns.org/data-sets/hc. They originate from the hippocampal subregion CA1 (three rats, HC2 [9]) and additionally the entorhinal cortex (EC) from another rat (HC4 [6]). Rats used for the HC-data sets were three to eight months old males, with a weight between 250 g and 400 g and deeply anesthetized with isoflurane (1-1.5 %) for implantation. The hippocampal signals were recorded during different behavioral tasks after the rats had one to two weeks to recover from the surgery. 32 – or 64 – site silicon probes were implanted into each rat‘s brain and recorded from CA1 in the right dorsal hippocampus. Rat 2 from the dataset HC4 additionally received another 4 - shank silicon probe implanted into the right dorso-caudal medial entorhinal cortex (EC2, EC3, EC5). All the protocols were authorized by the Institutional Animal Care and Use Committee of Rutgers University (protocol No. 90-042), at the time of recording and all experiments were performed at Rutgers University [10].

NES data was labeled into two classes, according to where the signals originated: in the cerebral cortex (CTX) or with a wide safety margin in the thalamus (THL). Recordings were fragmented into sequences of 5000 samples which corresponds to a time period of 1 second each. HC data was split into sequences of 5000 samples which corresponds with their 20 kHz sampling rate to a time frame of 0.25 seconds. Data set HC4 was partitioned in two and one part was used for training and one for testing only. HC2 was exclusively dedicated to testing. From the NES data set one rat was excluded from training and subsequently used exclusively for testing.

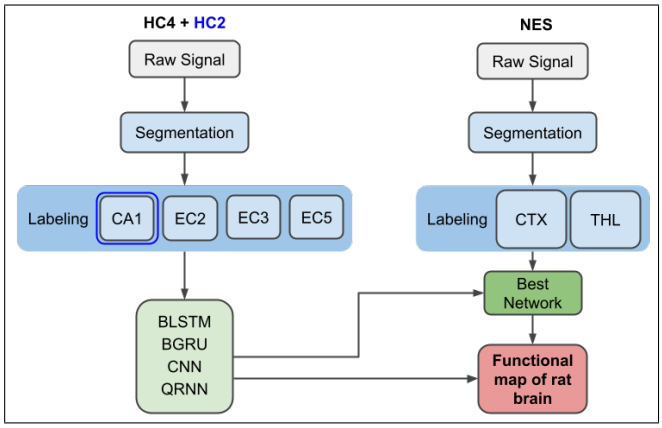

Fig. 3. Workflow overview: First, neural architectures were evaluated using the HC4 dataset. After the best performing network was identified, the HC2 dataset was used to validate these results. Finally, the best performing network was trained with the NES dataset and their performance with respect to different brain regions and a different dataset was evaluated.

C. Network Architectures

Several deep neural network architectures were implemented to find the most suitable network to classify the datasets according to their respective brain regions. A Bidirectional Long-Short Term Memory (BLSTM), a Bidirectional Gated Recurrent Unit (BGRU), a Quasi-Recurrent Neural Network (QRNN) and a Convolutional Neural Network (CNN) were implemented in PyTorch [11]. The results of the different models were compared to identify the most successful method. All networks receive a minimally filtered brain signal as input and are supposed to predict the associated brain region. Figure 3 shows the schematic diagram of the proposed workflow. Succesful signal-to-region classification might finally construct a functional map of the rat brain.

A BLSTM is thought to effectively solve time series classifications [12] as it remembers past states. It’s long-range dependencies make it suitable for pattern recognition in time signals. A BGRU contains fewer internal parameters than a BLSTM [13] and thus compares well in both training time and achieved accuracy for the task posed in this work. Recently CNNs are being used more frequently to analyze time series data [14], [15] extending their usual field of image datasets. Because of their faster training time and broader perspective, a CNN was added to the evaluation. Finally a QRNN, which can be seen as a mixture of a CNN and a RNN [16], was implemented and trained according to Figure 3. Table I lists some important hyperparameters of each architecture type used. The adjustment of the different hyperparameters was done manually for each individual architecture to reach the best possible performance for each network.

III. Results

According to our workflow, classification was first attempted on the hippocampal subregions contained in the HC data sets. The first row in Table II shows the achieved accuracy of the four networks networks implemented. The BGRU performed best with an accuracy of almost 89 % and clearly outperforms the other architectures. The LSTM and

TABLE I

COMPARISON OF DIFFERENT HYPERPARAMETERS OF THE BGRU, THE BLSTM, THE CNN, AND THE QRNN.

Architecture	Number of training input sequences	Batch Size	Number Epochs	Model Specifications
BGRU	204,800	16	2	2 hidden layer, size 64
BLSTM	204,800	16	2	2 hidden layer, size 256
CNN	1,684,998	128	20	5 Convolutional layers (kernel size 5) with output channels of size 50,75, 100, 125, 125 respectively
QRNN	1,443,520	128	2	3 hidden layers, size 256

TABLE II

COMPARISON OF A THE ACCURACY AND PER-CLASS F-MEASURE (AS PERCENTAGES) FOR THE DIFFERENT NETWORKS.

Testset HC4	class	BGRU	BLSTM	CNN	QRNN
accuracy	all	88.6	80.6	79.7	73.8
f-measure	CA1	95.4	90.0	93.7	91.0
	EC2	90.1	82.7	75.9	77.3
	EC3	83.8	71.2	70.4	59.8
	EC5	84.8	77.8	79.4	64.1

the CNN perform comparably with an accuracy of about 81 % and 80 %. With these values, both networks are about 10 % below the performance of the BGRU. The worst performing network is the QRNN with an accuracy of 74 % only. Looking at the f-measure of each class, it can be seen that the class CA1 is predicted best for every network. Even though the overall performance of the networks differ up to some 15 %, the prediction performance towards the class CA1 is nearly similar for all architectures and differs only up to 4.4 %. This indicates that the class CA1 contains properties that more strongly differentiate it from the other classes. It has to be noted, that none of the usual, electrophysiologic feature extraction steps have been attempted and only band pass filtering (f_L = 300Hz, f_H = 3kHz) was used.

Results from the best performing BGRU network and for the different data sets are shown in the following. The confusion matrix in Figure 4 displays the classification success on the dataset HC4. The prediction performance of the network is good, as indicated by the dark color along the diagonal axis.

Dataset HC2 was exclusively used for testing and was therefore not part of the training data. The only class present in this dataset is the subregion CA1 in the hippocampus. Dataset HC4 contains only recordings from the rat 2, whereas dataset HC2 contains recordings of the rats 1, 2 and 3. Therefore rat 2 data is present in both datasets. Table II summarizes the most important information about the performance of the different networks. This includes the overall accuracy according to the HC4 test set and the different neural network architectures. Additionally, the f-measure for each class of the HC4 test set is provided. The average accuracy of the BGRU regarding the

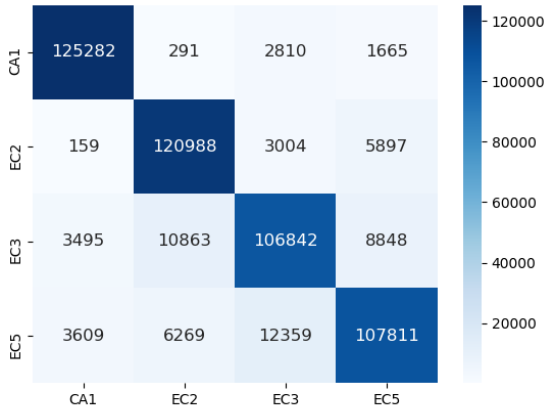

Fig. 4. Confusion matrix of the proposed bidirectional BGRU and the HC4 dataset.

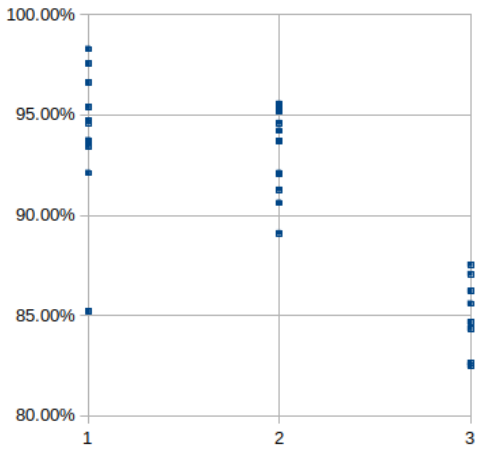

Fig. 5. Blue squares mark the accuracy of the BGRU with respect to the different recording sessions in the HC2 dataset (see [9] for details). Accuracy results for rats 1 to 3 are plotted on the x-axis and the accuracy of the network on the y-axis.

dataset HC2 is 91 %. Figure 5 shows the results of the BGRU for the HC2 dataset. The blue squares mark the classification accuracy across different recording sessions in the dataset. These results show that the BGRU works reasonably across rats and and behavioral situations.

With this intermediate result we tackled the more complex, yet artifact ridden NES data and tried to separate cortical (CTX) from thalamic (THL) signals (see Figure 6 left) along recording sites 1 mm lateral to midline (group 1) from 6 rats. Figure 6 right shows that no particular rat is classified substantially better than any other. Rat 2, whose data was not used for training, performs comparable to the others. We therefore conclude the learned properties of our BGRU to be able to make predictions for a wider range of rats.

Further classification of subregions within Cortex (orange), Thalamus (yellow), Hippocampus (brown) or Corpus Callosum (pink) (colors in Figure 6 left) goes beyond the work at hand and requires post-mortem validations of implant sites beyond the stereotaxic coordinates.

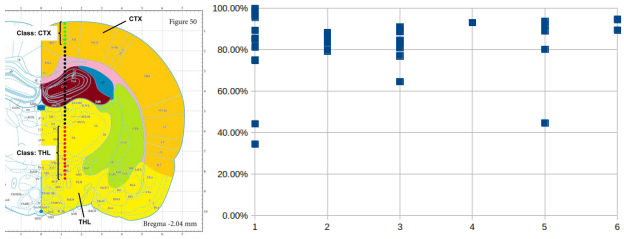

Fig. 6. (left) Illustration of the two most prominent anatomical regions in this hand-modified atlas slide [8]: cortical areas (CTX) in orange and thalamic areas (THL) in yellow. Training data originates from red and green dots. (right) Blue squares show the accuracy of the BGRU to seperate between CTX and THL data corresponding to the different recording sessions in the NES dataset. Rats 1 to 6 are plotted on the x-axis and the accuracy of the network on the y-axis.

IV. Conclusion

In this paper and as a first, we successfully mapped large data sets of extracellular recordings from different cortical depths and anatomical structures to their respective brain regions with the use of deep learning algorithms. Further development and rigorous histological cross-validation will build the basis to improve intraoperative targeting in preclinical animal research. This new application will advance bioelectronic medicine in its quest for maximum implantation accuracy as well.

The results are indicative of a strong connection between a spatial position in the brain, its neuro-anatomical make-up and extracellular recordings at least under controlled anesthetic conditions (here injection anesthesia). This connection is demonstrated for two major regions of the rat brain (CTX and THL) and some subregions within the hippocampus (CA1, EC2, EC3 and EC5) with the help of different deep learning network architectures.

Four different neural network architectures were successful in solving the classification task of actual neural signals according to the respective brain regions. The performance of the different networks varies and therefore the networks are differently well suited for solving the given task. The best performing network uses Gated Recurrent Units.

The results are also indicative that the predictive ability of the networks is not animal-specific. The BGRU was trained with signals from one rat in the HC4 dataset but was able to predict the region CA1 for two other rats with a high accuracy. The same is true for the NES dataset and the BGRU, which was trained with recordings from five individual rats and successfully tested with signals from another rat. This raises hopes that a BGRU can be trained once and then be used online for different animals without the need for re-training.

Further research in this area is needed to actually compile a useful, detailed and voluminous functional atlas and apply its localization power to laboratory research and pre-clinical neurosurgery. The creation of a dataset with an additional histological validation will provide a reliable targeting of every brain region. Data sets that include reliable identification of all available brain regions in animal models will provide insight into whether the creation of a functional map might become a possibility for the entire human brain. Here, many more factors that could influence the classification performance, such as age, diseases, gender, and anesthesia type, need to be investigated as well. This work forms a basis for a brain region identification with deep learning and shows that artificial neural networks, such as the BGRU, are able to solve such tasks.

Acknowledgment

We are grateful to György Buzsáki's lab for generously sharing the hippocampal data. Algorithms and NES data will be made available upon reasonable request.

References

[1] S. Treu, B. Strange, S. Oxenford, W.-J. Neumann, A. Kühn, N. Li, and A. Horn, "Deep brain stimulation: Imaging on a group level," *Neuroimage*, vol. 219, p. 117018, 2020.

[2] L. Ramrath, S. Vogt, W. Jensen, U. G. Hofmann, and A. Schweikard, "Computer- and robot-assisted stereotaxy for high-precision small animal brain exploration," *Biomedizinische Technik / Biomedical Engineering*, vol. 54, pp. 8–13, 2009.

[3] L. W. Swanson, "Brain maps 4.0—structure of the rat brain: An open access atlas with global nervous system nomenclature ontology and flatmaps," *J Comp Neurol.*, vol. 526, pp. 935–943, 2018.

[4] C. K. Moll, A. Struppler, and A. K. Engel, "Intraoperative Mikroelektrodenableitungen in den Basalganglien des Menschen," *Neuroforum*, vol. 1, pp. 11–20, 2005.

[5] A. Sayed Herbawi, O. Christ, L. Kiessner, S. Mottaghi, U. G. Hofmann, O. Paul, and P. Ruther, "CMOS neural probe with 1600 close-packed recording sites and 32 analog output channels," *Journal of Microelectromechanical Systems*, vol. 27, pp. 1023 – 1034, 2018.

[6] K. Mizuseki, A. Sirota, E. Pastalkova, G. Buzsáki, and A. Peyrache, "Extracellular recordings from multi-site silicon probes used for clustering of neuron responses in rat hippocampal and entorhinal regions." *CRCNS - Collaborative Research in Computational Neuroscience - Data sharing*, 2014.

[7] A. Richter, Y. Xie, A. Schumacher, S. Löffler, R. D. Kirch, J. Al-Hasani, D. H. Rapoport, C. Kruse, A. Moser, V. Tronnier, S. Danner, and U. G. Hofmann, "A simple implantation method for flexible, multisite microelectrodes into rat brains," *Frontiers in Neuroengineering*, vol. 6, p. 6, 2013.

[8] G. Paxinos and C. Watson, *The Rat Brain in Stereotaxic Coordinates*. Academic Press, San Diego, 2005.

[9] K. Mizuseki, A. Sirota, E. Pastalkova, and G. Buzsáki, "Multi-unit recordings from the rat hippocampus made during open field foraging." *CRCNS - Collaborative Research in Computational Neuroscience - Data sharing*, 2009.

[10] K. Mizuseki, K. Diba, E. Pastalkova, J. Teeters, A. Sirota, and G. Buzsáki, "Neurosharing: large-scale data sets (spike, lfp) recorded from the hippocampal-entorhinal system in behaving rats," *F1000Research*, vol. 3, p. 98, 2014.

[11] A. Paszke, S. Gross, F. Massa, A. Lerer *et al.*, "PyTorch: An imperative style, high-performance deep learning library," in *Advances in Neural Information Processing Systems 32*, 2019, pp. 8024–8035.

[12] Y. Hua, Z. Zhao, R. Li, X. Chen, Z. Liu, and H. Zhang, "Deep learning with long short-term memory for time series prediction," *IEEE Communications Magazine*, vol. 57, pp. 114–119, 2019.

[13] S. Yang, X. Yu, and Y. Zhou, "LSTM and GRU neural network performance comparison study: Taking yelp review dataset as an example," *Int. Workshop on Electr. Comm. and Artificial Intelligence (IWECAI)*, pp. 98–101, 2020.

[14] H. I. Fawaz, G. Forestier, J. Weber, L. Idoumghar, and P.-A. Muller, "Deep learning for time series classification: a review," *Data Mining and Knowledge Discovery*, vol. 33, no. 4, p. 917–963, 2019.

[15] B. Zhao, H. Lu, S. Chen, J. Liu, and D. Wu, "Convolutional neural networks for time series classification," *Journal of Systems Engineering and Electronics*, vol. 28, no. 1, pp. 162–169, 2017.

[16] J. Bradbury, S. Merity, C. Xiong, and R. Socher, "Quasi-recurrent neural networks," *arXiv:1611.01576v2*, 11 2016.